ASSOCIAZIONE NAZIONALE ITALIANA DI INGEGNERIA SISMICA
ANIDIS
Italian National Association of Earthquake Engineering

XVIII CONVEGNO ANIDIS
L'ingegneria sismica in Italia
ASCOLI PICENO 2019
15-19 Settembre

Una tecnologia integrata isolamento-scorrimento alla base per il controllo del taglio sismico degli edifici

Francesca Barbagallo[a], Melina Bosco[a], Edoardo Michele Marino[a], Pier Paolo Rossi[a], Antonino Russo[a]
[a] *Dipartimento di Ingegneria Civile e Architettura, Università degli studi di Catania, Via Santa Sofia, 64, 95123 Catania*

Keywords: existing RC frame; seismic retrofit; base isolation; base shear capping; sliding.

ABSTRACT
The seismic upgrading of existing r.c. buildings has become a pressing need, especially in the Mediterranean area. Indeed, the majority of the building stock is not able to sustain seismic actions, because it was conceived and designed to sustain gravity loads only, or for seismic actions lower than those expected from the current seismic zonation. A large variety of retrofit techniques has been developed and proposed during the last decades, among which the base isolation is deemed as one of the most effective. In fact, it is able to reduce the seismic force acting on the structure. Unfortunately, the seismic demand of the structure keeps increasing with the input magnitude. More recently, another possible retrofit intervention has been proposed by detaching the structure from the foundation to let the structure slide in case the seismic force overcomes the friction force. This intervention is able to cap the base shear of the superstructure to a value that is independent of the input magnitude. The main drawback is that the maximum value of the base shear can be significantly larger than the friction force and may overcome the structural resistance. Based on this background, this paper aims to explore the possibility of a new retrofit technique, named "isoslider". This technique integrates the conventional base isolation technology with the sliding system. The goal is to compensate the deficiencies of the two technologies by exploiting their positive features. Indeed, on one hand the slider should cap the shear force in the structure to a value independent of the input magnitude, on the other hand the base isolation should reduce the amplification of the shear capping with respect to the friction force." In this paper a design procedure of the isosliding system is proposed and the seismic behaviour of the isosliding system is investigated and compared to that of a fixed base structure, a base isolated structure and a sliding structure. To this end, a simplified two degree of freedom model was analysed by means of incremental nonlinear dynamic analysis.

1 INTRODUCTION

The majority of the European building heritage was designed in the past decades neglecting the effects of seismic excitation, or according to obsolete seismic design provisions. As a consequence, many existing buildings suffer from seismic deficiencies and are extremely vulnerable to the seismic action. The vulnerability of the existing building stock is a serious concern that is gaining increasing attention within the research community as well as the public society. Indeed, in order to mitigate the seismic risk of existing structures and to enhance the structural safety against earthquakes, seismic retrofit is necessary [Pampanin, 2006]. Because of this, the scientific community has been devoting great efforts to develop innovative seismic upgrading solutions. Out of the retrofit techniques that are today available, base isolation of structures is deemed as one of the most effective [Warn and Ryan, 2012]. It requires the introduction of isolators, generally located at the base of the first storey columns. The addition of the base isolation increases the fundamental period of the structure, thus reducing the seismic force acting on the structure [Cardone et al, 2012]. Several researches have worked on base isolation and proved the effectiveness of this technology in reducing the vulnerability not only of r.c. buildings but also of historical buildings [De Luca et al, 2011; Matsagar and Jangid, 2008, Tomazevic et al, 2009].The main drawback of the base isolation stems from the fact that the base

shear exerted on the superstructure grows with the magnitude of the seismic input. Thus, in case of unexpected strong earthquakes, the base shear may reach large values and the isolators may undergo deformations that could exceed their capacity.

As an alternative to the conventional base isolation, scientific researches proposed the introduction of a sliding system at the base of the structure. In this approach, the superstructure is detached from the foundation and allowed to slide in case the base shear overcomes the friction force [Mostaghel and Tanbakuchi, 1983; Younis and Tadjbakhsh, 1984; Mohamad et al, 2015]. Owing to the sliding, the shear forces on the superstructure are controlled by the friction coefficient of the sliding surface. Previous studies [McCormick et al, 2009; Enokida et al, 2015] explored the possibility to lubricate the sliding mortar surface with graphite powder to achieve a proper friction coefficient. The main advantage offered by the sliding system is that it is able to cap the base shear of the upper structure to a maximum value that does not depend on the magnitude of the earthquake. Furthermore, this approach does not require any special devices or construction works. Unfortunately, the effectiveness of this system is undermined by the fact that the maximum value of the base shear force exerted on the upper structure is larger than the friction force, and it may reach values that are even 2.5 times larger than the friction force [Barbagallo et al, 2016; Barone 2017]. This is caused by a dynamic amplification of the friction force that acts on the mass at the base of the structure. Because of this, the base shear in the upper structure could overcome the resistance of the structure, thus compromising the retrofit intervention.

To overcome the drawbacks of both the base isolation and the sliding system, this paper explores a joined technology, named “Isosliding”, whereby isolators are introduced at the base of columns and are let free to slide on a lubricated surface. The goal is to exploit the strength points of the two technologies to defeat their weaknesses. On the one hand, the use of the Isosliding system should allow the control of the base shear in the upper structure owing to the sliding, regardless of the seismic magnitude. On the other hand, the low lateral stiffness of the isolator should reduce the dynamic amplification of the friction force, thus helping to keep the base shear below the resistant capacity of the structure.

The goals of this paper are to (i) develop a design procedure to determine the properties of the isolators that have to be combined with the sliding system and (ii) compare the seismic response provided by the Isosliding to that obtained by the conventional base isolation, the sliding system and the simply fixed base structure. To this end, incremental nonlinear dynamic analyses were conducted on a simplified two degrees of freedom numerical model.

2 NUMERICAL MODELS

The following numerical models were built using the Opensees software [Mazzoni et al., 2003] in order to (i) analyse the dynamic amplification of the friction force in the system with slider, (ii) develop a design procedure of the isoslider, (iii) compare the seismic response of the isosliding system to that of its counterparts, i.e. the fixed base structure, the sliding structure and the base isolated structure. Four numerical models are developed to simulate four different structural systems: the fixed base structure (1), the base isolated structure (2), the sliding structure (3) and the isosliding system (4), as shown in Figure 1. All the numerical models are two Degrees Of Freedom (2DOF) systems with two lumped masses. To be representative of a six storey high r.c. frame, the total mass of each structure is assumed equal to 848 *t*, considering the mass of a generic storey equal to 127.8 t. Given six storeys in the upper structure and considering the additional deck in correspondence of the foundation, the mass ratio, i.e. the ratio of the mass of the upper structure to the total mass, is 0.85. Hence, the upper mass m_1 and the lower mass m_2 are equal to 724.2 *t* and 127.8 *t*, respectively. These masses are connected by a zero length element, whose stiffness is assigned so that the fundamental period of the fixed base structure is 0.2 s. The fixed base structure was

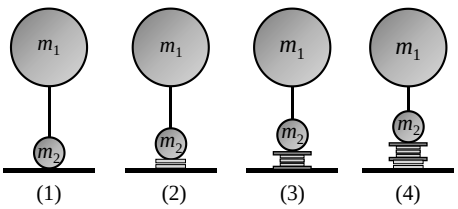

Figure 1. Numerical models: (1) fixed base structure, (2) sliding structure, (3) base isolated structure, (4) structure with isoslider system

simulated by fixing the lower mass to the ground. For the base isolated structure, the sliding structure and the structure with the isosliding system an additional element was introduced between the lower mass and the ground. For the base isolated structure, an elastomeric rubber bearing was supposed to be used. This is characterized by an elastic plastic hardening behaviour (Figure 2a), where D is the maximum displacement capacity of the bearing, D_y is the displacement corresponding to the yielding of the bearing, Q is the force given by the intersection between the plastic branch and the y axis, K_{eff} is the effective stiffness of the bearing, K_1 and K_2 are the elastic stiffness and the stiffness of the plastic branch, respectively. The value of K_1 and K_2 depends on the type of bearing and in the case of elastomeric rubber bearing the ratio K_1/K_2 was assumed equal to 10 [Naeim and Kelly, 1999]. The rubber bearing was modelled by means of the elastomeric bearing plasticity element available in the OpenSees library. This element was added between the lower mass and the node corresponding to the ground. Both the axial and flexural stiffness of the bearing are assumed very large, while the elastic stiffness K_1, the yielding force f_y and the post yielding stiffness ratio are those determined by the design procedure. A further mass m_3 is lamped below the elastomeric bearing to simulate the mass of the bearing, and is taken equal to 1/200 of the total mass

To model the sliding structure, the flat sliding bearing element is introduced between the lower mass m_2 and the ground. This element has an elastic perfectly plastic behaviour (Figure 2b). The maximum resistance of the element is the friction force f_μ and the sliding starts when the horizontal force equals the friction force. The friction coefficient is set equal to 0.16 [Barbagallo et al, 2016] and its value is constant according to the Coulomb friction model. A large elastic stiffness k_1 is assigned and is determined so that when the horizontal force equals the friction force and sliding begins, the lateral displacement of the slider is 0.05 mm. The axial stiffness is assumed extremely large to prevent axial deformation, while the flexural stiffness is extremely low to allow the rotation of the column base.

The numerical model of the structure with the isoslider joins the flat slider bearing element (connecting the ground to the base of the rubber bearing) and the elastomeric bearing plasticity element (connecting the base of the rubber bearing to the base of the column).

Rayleigh viscous damping was adopted with the equivalent viscous damping ratio of 5% assigned to two main periods of vibration, T_1 and T_2. In the sliding structure (model 2) T_1 was that of the fixed base structure T_{fix} and T_2 was that of the structure during the sliding phase, evaluated as function of the mass ratio α

$$T_2 = T_{fix} \cdot \sqrt{1-\alpha} \qquad (1)$$

In the base isolated structure (model 3), T_1 was the period of vibration of the base isolated structure evaluated considering its secant stiffness K_{eff}, while T_2 was assumed equal to T_{fix}, following the suggestion of the Italian code for the base isolated structures [NTC 2018]. In the case of the structure with isoslider, T_1 was the period of vibration corresponding to the secant stiffness K_{eff}, and T_2 was that of the sliding structure evaluated by Eq. 1. Finally, the damping matrix of the fixed base model was assumed as that of the sliding system.

3 BACKGROUND: DYNAMIC AMPLIFICATION OF THE BASE SHEAR IN THE SLIDING STRUCTURE

The sliding system requires the separation of the column base of the first level from the foundation, as shown in Figure 3. The column

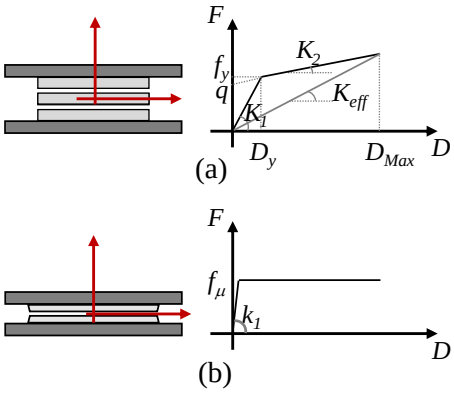

Figure 2. Numerical model of (a) base isolation and (b) slider

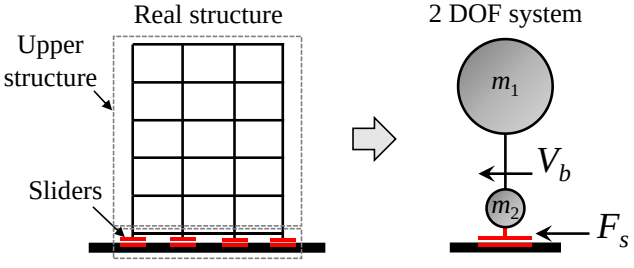

Figure 3. Concept of the sliding system and 2DOF system

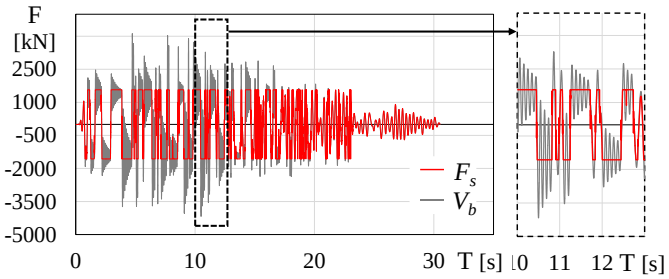

Figure 4. Time history of the base shear in the upper structure and the friction force in the slider

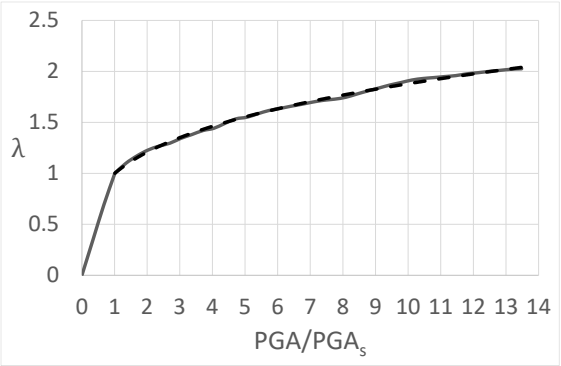

Figure 5. Time history of the base shear in the upper structure and the friction force in the slider

bases slip on the sliding surface, which is characterised by its own friction coefficient. Between the column base and the sliding surface the friction force develops. As a consequence, the structure is simplified as the model (2) previously introduced. If the horizontal force caused by the seismic action is lower than the friction force, the structure behaves as fixed base (stick phase). When the seismic action overcomes the friction force, the structure slides towards one direction (sliding phase) and stops only when the horizontal force reduces again below the friction force. Hence, during the input motion, the sliding structure alternates the stick phase and the sliding phase, and may change sliding direction when shifting from one to the other phase. In order to investigate the dynamic behaviour of a generic sliding system, a 2 degree of freedom (DOF) model with a total mass of 100 *t* and a ratio of the upper mass over the total mass α equal to 0.9 was assumed as an example. The sliding surface was supposed to have a friction coefficient equal to 0.16, representative of the graphite powder lubrication of the sliding surface. Hence, the friction force is equal to 1569.6 kN. This numerical model is subjected to an input motion with Peak Ground Acceleration (PGA) equal to 2.0 *g*. The details about the input motion are reported in sections 5. Figure 4 shows the time history response of the reaction force of the slider F_s (red line) and the base shear of the upper structure V_b (grey line). During the sliding phase, the reaction force reaches its maximum value (+/- 1569.6 kN) and remains constant. Meanwhile, the shear force V_b transmitted to the upper structure oscillates around the value of the friction force and may reach values (4168 kN, in this example) significantly larger than the friction force. The ratio of the shear force in the upper structure to the friction force is here defined as amplification λ.

Incremental nonlinear dynamic analyses were conducted on the example model and the seismic input was applied with PGA ranging from 0.05 *g* to 2.0 *g*. Figure 5 shows that the maximum value of the amplification λ increases with the magnitude of the seismic input up to 2.0-2.5 times the friction force [Barone, 2017]. This phenomenon came to light also in the experimental results provided by shaking table tests [Barbagallo et al., 2016].

A physical explanation to this phenomenon is here provided based on two considerations. First, it is analytically demonstrated [Chopra, 1995] that a suddenly applied force (step force) produces twice the deformation (and elastic reaction force) it would have caused if the same force was applied as a static force. This is also the case of the sliding system. In fact, when sliding begins, the friction force is suddenly exerted on the foundation mass and remains constant until the structure sticks again to the ground. Hence, the step force is the friction force, the mass is that of the foundation, and the reaction force is the base shear of the upper structure. Second, every time the structure starts to slide towards the opposite direction, the friction force applies as a step force on a mass that is already moving, thus leading the base shear in the upper structure to a value that may be even larger than twice the friction force.

4 DESIGN PROCEDURE OF THE ISOSLIDING SYSTEM

The design procedure of the isosliding structure has two main goals: (i) capping the base shear of the structure to a value lower than that corresponding to the structural collapse and (ii) maintaining the horizontal displacement of the isolators below the capacity. The design procedure is ruled by four parameters: the friction coefficient μ of the sliding surface, the PGA corresponding to the start of the sliding, the

displacement capacity D and the equivalent viscous damping β of the isolators. The design procedure is summarized in the flowchart shown in Figure 6. The value of the friction coefficient depends on the treatment used for the sliding surface. In this study, the surface is supposed to be lubricated by graphite powder, which provides a stable friction coefficient equal to 0.16 [Barbagallo et al. 2016]. The PGA corresponding to the start of sliding is here assumed equal to 0.35 g, which is the one stipulated for the verification of the Significant Damage (SD) limit sate in EC8 in high seismicity zone. The maximum displacement capacity of the isolators depends on the type of isolator adopted and is provided by the producers. For this study, a rubber bearing was used and its capacity D was found to be equal to 200 mm. However, to prevent the collapse of the bearing at the occurrence of sliding (i.e. at PGA = 0.35 g), the design displacement D_d capacity of the bearing is taken as a fraction of D. In particular, D_d is evaluated by dividing the displacement capacity D by 1.71, that is the ratio of the PGA corresponding to the Near Collapse limit state and that corresponding to the Significant Damage limit state. Hence, the effective stiffness K_{eff} of the rubber bearing is calculated dividing the friction force F_μ by D_d, F_μ being the product of

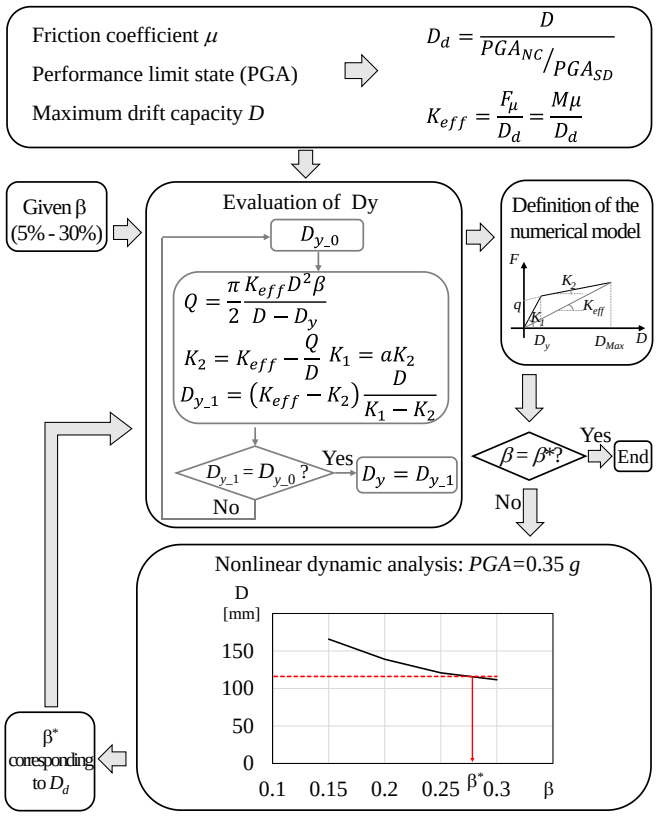

Figure 6. Design procedure of the isoslider

the friction coefficient μ times the weight of the structure.

With regards to the equivalent viscous damping, this was not fixed preliminarily, but it was specifically determined as that value (β*) corresponding to the attainment of the capacity D_d of the bearing when the PGA causes the start of sliding, i.e. 0.35 g. To this end, several tentative values of β were adopted, ranging from 5% to 30%, in step of 5%. Given the value of β, the displacement D_y corresponding to the yielding of the bearing was determined by means of the iterative procedure shown in Figure 6 [Naeim and Kelly, 1999]. Hence, all the parameters needed for the determination of the corresponding numerical model of the bearing were determined and nonlinear dynamic analysis were conducted on the numerical model (3). A set of ten artificial accelerograms was applied and scaled to a PGA = 0.35 g. Hence, the maximum displacement recorded during each accelerogram was averaged over ten accelerograms and corresponded to a fixed value of β. This procedure was repeated for every tentative value of β, thus leading to the D-β curves shown in Figure 6. The value of β^* was determined by the intersection between the curve corresponding to 0.35 g and the displacement capacity D_d of the bearing. Given β^*, the corresponding value of D_y^* was determined according to the same procedure shown before and the design of the isolator was completed.

5 NUMERICAL ANALYSIS

Incremental nonlinear Dynamic Analyses (IDA) were conducted to investigate how the insertion of the slider, the isolator, or the isoslider influence the seismic response of the structure. Furthermore, the nonlinear dynamic analyses allowed the validation of the design procedure of the isoslider. To this end, the four abovementioned numerical models were subjected to a set of 10 artificial ground motions. These accelerograms were compatible with the EC8 elastic spectrum for soil type C characterized by 5% damping ratio and reference PGA equal to 0.35 g. The seismic inputs were generated by SIMQKE computer program [SIMQKE, 1976] so that the mean spectrum in terms of acceleration (Figure 7) was compatible with the response spectrum proposed by EC8 in Appendix A. Each ground motion has a total duration of 30.5 s and

is enveloped by a three branch compound function: (1) an exponential increasing function, (2) a constant function (strong motion phase) and (3) a function with exponential decay [Amara et al., 2014]. The duration of the strong motion phase is 7.0 s. The IDA was conducted by increasing the PGA from 0.05 *g* to 2.0 *g* in step of 0.05 *g*.

The seismic response of each of the four numerical model was analysed with reference to the following response parameters: the base shear of the upper structure, the base shear of the isolator and that of the slider; the drift demand of the isolator, sliding displacement of the structure. For every PGA and for each of the 10 ground motions, the maximum values during the time history of each response parameter was recorded. Hence, following the recommendation of EC8, the mean over the 10 accelerograms is calculated for each response parameter.

6 EFFECTIVENESS OF BASE ISOLATION, SLIDER OR ISOSLIDER

Figure 8 compares the shear force demands for increasing PGA of the analysed systems. In particular, the shear force of the fixed base system (model 1) is reported in Figure 8 (a) alongside with that in the upper structure of the systems with slider (model 2), base isolation (model 3) and isoslider (model 4). Furthermore, in this figure, the dashed grey line plots the value of the friction force. Instead, Figure 8 (b) compares the shear force demand in the isolator of the models 2 and 3. In both the aforementioned figures, the dashed-dotted blue line identifies results of model 1 while continuous lines with different colours identify the results of models 2, 3 and 4.

Figure 8 (a) shows that, for a given value of PGA, the three retrofit techniques here considered share one common feature, i.e. they are able to reduce the shear force in the upper structure compared to the fixed base structure. However, each technique offers a different seismic response. Before the sliding phase, the structure with the slider and the fixed base structure have almost the same elastic stiffness, that is larger than that of the structure with base isolation or isoslider. With regards to the base isolation, the shear force in the upper structure increases with the input magnitude. The rate of increase of the shear force is lower than that of the fixed base system, but there is not an upper limit of the shear force. When the slider is inserted and the sliding has occurred, the shear force in the upper structure increases with the input magnitude, but the rate of increase is significantly lower than that of the fixed base system and tends asymptotically to an upper value. In this phase, the rate of increase of the shear force of the sliding system is also lower than that of the system with base isolation. The insertion of the isoslider at the base of the structure virtually allows the capping of the base shear in the upper structure. Indeed, in the sliding phase, the shear force in the upper structure increases very slowly with PGA and becomes just 5% and 20% larger than the friction force for PGA values of 1.0 and 2.0 g, respectively. The shear force of the upper structure of the system with isoslider is lower

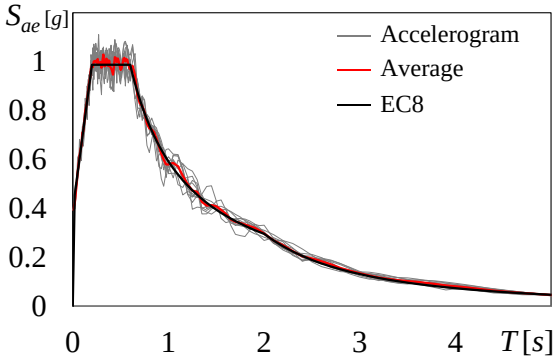

Figure 7. Elastic response spectra of the 10 accelerograms, average elastic response spectrum, EC8 response spectrum.

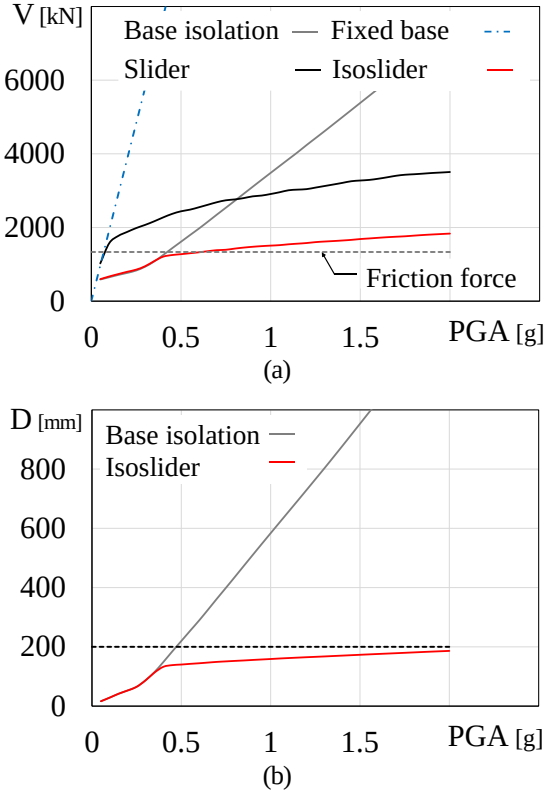

Figure 8. Shear force demand in (a) the upper structure and (b) base isolation.

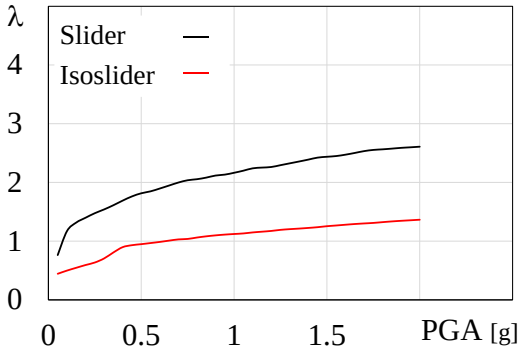

Figure 9. Coefficient of amplification λ

than that recorded in the other analysed systems in the entire range of PGA, which denotes that the isoslider provides the best protection of the upper structure. Furthermore, the isoslider allows the reduction of the shear force exerted on the isolator, as shown in Figure 8 (b).

One of the targets of the system with isoslider is the reduction of the amplification λ of the friction force with respect to the system with slider. Figure 9 plots the value of λ both in the sliding structure and the isosliding structure and shows that, even for very strong earthquakes, the shear force in the superstructure of the isosliding system is capped to values slightly larger than the friction force, while in the case of the sliding structure the shear force rapidly attains values twice larger than the friction force.

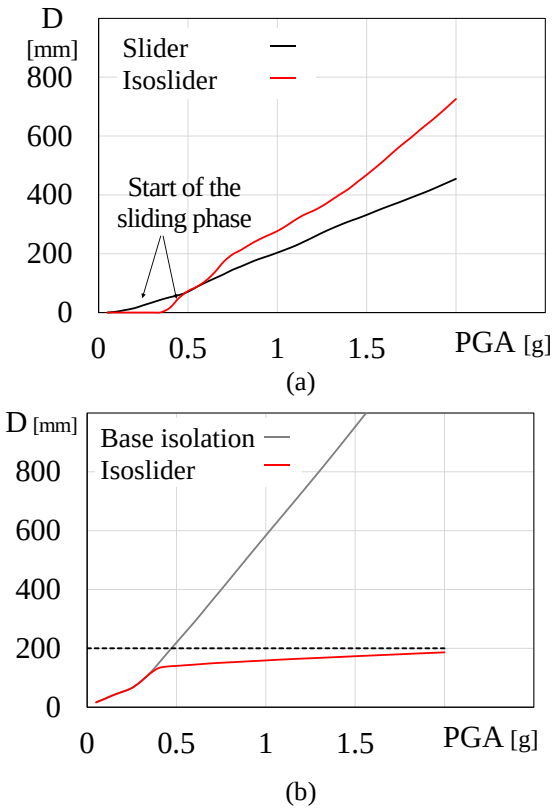

Figure 10. (a) Sliding displacement in the structure with slider and isoslider, (b) drift demand in the isolator of the base isolated structure and the isosliding structure.

Figure 10 (a) plots the displacement developed by the base of the structure with the slider and that with the isoslider. The structure with the slider starts to slide for a PGA lower than 0.1 *g*, while in the case of the isoslider the sliding is postponed and occurs at PGA = 0.35 *g*. This results is consistent with the design procedure, whereby the PGA corresponding to the sliding phase was set equal to 0.35 *g*, and promotes the system with isoslider over the system with slider from the point of view of serviceability verification in occurrence of moderate earthquakes. The displacement attained by the two structural systems is comparable, even though in some cases the isoslider may lead to a larger displacement compared to the slider. However, it should be noted that this is the case of extremely strong input magnitude. Furthermore, the isoslider is able to reduce the displacement demand of the isolator, as shown in Figure 10 (b). Indeed, the displacement demand of the isolator increases with the PGA. However, when the isoslider is used (red line) and the system starts to slide, the rate of increase of the displacement demand of the isolator becomes significantly lower than that of the base isolated structure (grey line). Indeed, even for extremely large PGAs, the isolator of the isoslider does not reach its maximum capacity (in this case set equal to 200 mm). On the contrary, in the base isolated system, the displacement demand of the isolator overcomes its capacity for a PGA close to 0.5 *g* and does not satisfy the near collapse performance objective of EC8, according to which the near collapse limit state should not be exceeded for PGA = 0.6 *g*.

7 CONCLUSIONS

This paper explores the possibility of a retrofit technique that integrates the conventional base isolation to the sliding system named isoslider. It is composed of a rubber bearing that is inserted at the base of the columns of the first level and it is let free to slide on a surface lubricated with graphite powder. A design procedure is proposed to determine the properties of the isolator. The design method is ruled by four parameters, i.e. the friction coefficient of the sliding surface, the PGA corresponding to the occurrence of the sliding, the displacement capacity and the equivalent viscous damping of the isolator.

To investigate the effectiveness of the design procedure and the seismic response of the structure provided with the isoslider, a simplified two degree of freedom system was analysed. The properties of the numerical model aimed to be representative of a six storey r.c. frame. Incremental nonlinear dynamic analysis were conducted, and the seismic response of the structure with isoslider was determined in terms of shear force in the upper structure and in the isolator, sliding displacement of the structure and displacement demand of the isolator. Furthermore, the seismic response thus obtained was compared to that of the structure with the fixed base, the base isolation and the sliding base. The numerical analyses show that the isoslider is able to cap the base shear in the superstructure to a value that is almost independent of the input magnitude. Indeed, the rate of the increase of the base shear with the PGA is extremely low and it is significantly lower than that of the sliding structure. Furthermore, the value of the base shear in the structure is nearly equal to the friction force, and the coefficient of amplification is close to 1. This means that the addition of the isolator allowed the reduction of the friction force amplification that developed in the structure with the slider. The introduction of the isoslider was effective also in terms of displacement. In fact, the displacement demand of the bearing remained below its capacity even for strong earthquakes. On the contrary, the same isolator used as classical base isolation would not have satisfied the Near Collapse limit state prescribed by EC8, because the displacement demand would have overcome the capacity for a PGA lower than 0.60 g. Finally, the design procedure allowed also to control the beginning of the sliding. Indeed, when the structure was provided with the isoslider, the sliding phase was postponed compared to the case of the slider and it started at 0.35 *g*, as set in the design procedure.

8 REFERENCES

Pampanin S., 2006. Controversial aspects in seismic assessment and retrofit of structures in modern times: understanding and implementing lessons from ancient heritage, *Bulletin of the new zealand society for earthquake engineering*, **39**, 2.

Warn G.P., Ryan K. L., 2012. A review of seismic isolation for buildings: historical development and research needs. *Buildings*, **2**, 300-325;

Cardone D. Flora A., Gesualdi G., 2012. Inelastic response of RC frame buildings with seismic isolation. *Earthquake Engineering and Structural Dynamics*, **42**, 6, 871-889

De Luca A., Mele E., Molina J., Verzeletti G., Pinto A. V., 2001. Base isolation for retrofitting historic buildings: Evaluation of seismic performance through experimental investigation. *Earthquake Engineering & Structural Dynamics*, **30**, 1125-1145.

Matsagar V., Jangid R.S.,2008. Base isolation for seismic retrofitting of structures. *Practice Periodical on Structural Design and Construction*, **13**, 175-185.

Tomazevic M., Klemenc I., Weiss P., 2009. Seismic upgrading of old masonry buildings by seismic isolation and CFRP laminates: a shaking-table study of reduced scale models. *Bullettin of Earthquake Engineering*, **7**, 1, 293–321.

Mostaghel N., Tanbakuchi J., 1983. Response of sliding structures to earthquake support motion. *Earthquake Engineering and Structural Dynamics* ,**11**: 729-748

Younis C., Tadjbakhsh I., 1984. Response of sliding rigid structure to base excitation. *Journal of Engineering Mechanics*, **110**: 417-432

Mohamad M. E., Ibrahim I. S., Abdullah R., Abd. Rahaman A.B., Kueh A. B. H., Usman J.,2015. Friction and cohesion coefficients of composite concrete-to-concrete bond. *Cement & Concrete Composites*; **56**: 1-14

McCormick J., Nagae T., Ikenaga M., Zhang P., Katsuo M., Nakashima M., 2009. Investigation of the sliding behaviour between steel and mortar for seismic applications in structures. *Earthquake Engineering and Structural Dynamics*; **38**: 1401-1419

Enokida R., Inami M., Nakashima M., Nagae T., Ikenaga M., 2012. Development of Free-Standing Steel structure using kinematic friction of steel-mortar. *15th World Conference on Earthquake Engineering*, Lisbon, Portugal.

Barbagallo F., Hamashima I., Hu H., Kurata M., Nakashima M., 2016. Base shear capping buildings with graphite-lubricated bases for collapse prevention in extreme earthquakes, *Earthquake Engineering & Structural Dynamics*, **46**, 1003-1021.

Barone R., 2017. Adeguamento sismico di edifici in c.a. tamponati mediante sistemi a scorrimento lubrificati (Seismic upgrading of RC framed buildings with infills by lubricated sliding base systems), *Thesis for Master Degree in Structural and geotechnical engineering*, (in Italian) University of Catania.

Naeim F., Kelly J. M., 1999. *Design of seismic isolated structures*, John Wiley and sons.

D.M. 17/01/2018. Norme Tecniche per le costruzioni (Provisions for constructions). Rome, 2018. (in Italian)

Mazzoni S., McKenna F., Scott M. H., Fenves G. L., Jeremic B., 2003. OpenSees command Language Manual, Pacific Earthquake Engineering Research Center, University of California at Berkely, USA.

Chopra A.K., 1995. Dynamics of structures: Theory and application to earthquake engineering", Prentice Hall, USA.

SIMQKE. A program for artificial motion generation, User's manual and documentation, Department of Civil Engineering MIT, 1976.

Amara F., Bosco M., Marino E.M., Rossi P.P., 2014. An accurate strength amplification factor for the design of SDOF system with P-Δ effects, *Earthquake Engineering and Structural Dynamics*, **43**: 589-611.